THE PENNSYLVANIA STATE UNIVERSITY
SCHREYER HONORS COLLEGE

DEPARTMENT OF MATERIALS SCIENCE AND ENGINEERING

# Studying the Influence of a Particle in the Liquid-Liquid Interface

LEONARDO BATISTA CAPAVERDE SILVA
SPRING 2022

A thesis
submitted in partial fulfillment
of the requirements
for a baccalaureate degree
in Materials Science and Engineering
with honors in Materials Science and Engineering

Reviewed and approved* by the following:

Lauren Zarzar
Assistant Professor of Chemistry
Thesis Advisor

Robert Allen Kimel
Associate Teaching Professor of Materials Science and Engineering
Honors Advisor

* Electronic approvals are on file.

# ABSTRACT

From the mixture of the ingredients in salad dressing to the several different components in the blood stream, there are multiple liquid-liquid interface interactions in our daily lives. One less studied approach to stabilize these different components is the use of colloidal particles in the liquid-liquid interface to decrease the contact area between the two liquids, lowering the interfacial energy of that system. This work is divided into two main sections. In the first study, the creation of a stable (for more than 2 months) double oil-oil emulsion in water is explored through the creation of silica particles with hydrophobic and hydrophilic end groups, allowing more configuration possibilities for droplet shapes in that system. In the second study, the droplet speed enhancement upon particle addition in the oil-surfactant solution is investigated, with droplet speeds reaching up to 300 μm/s with a 0.5 wt% silica particle in Triton-X, corresponding to a more than double speed increase. Although the exact mechanism is unknown, the results point to the permanent asymmetry of the droplet leading to enhancement of the Marangoni flow. A better understanding of the mechanisms of the phenomena was achieved, which can be of use in future research in the field.

# TABLE OF CONTENTS

# LIST OF FIGURES

# LIST OF TABLES

# ACKNOWLEDGEMENTS

I would like to thank Dr. Lauren Zarzar for accepting me into her lab in my first year as an undergraduate student. Without her support and continuous effort, I would not be able to excel in my research and go to pursue a Ph.D. A big thanks to all the graduate students in Dr. Zarzar's lab for welcoming me and explaining me all their research multiple times until I finally understood the concepts. Especially Seongik Cheon, who was the best research partner I could have hoped for. If in my graduate studies I become half a researcher as you, I will already have been successful.

I couldn't include my research with Dr. Maria Molina Higgins because it had no relation with the one presented in this thesis. Regardless, it was a wonderful experience, and I am grateful for her dedication to put me as a poster presenter in the TMS conference. It was a completely different experience, and it would not have been possible without our dedication and passion for sustainability.

I also extend my gratitude to all the professors (with a special mention to Dr. Kimel and Dr. Dabo for providing me letters of recommendation) and Penn State lab spaces, structures, and resources. This undergraduate experience was beyond my expectations and changed me professionally and personally like no other period of my life.

All of this could only be possible due to the efforts of my family, who financially and emotionally supported me throughout my journey, so I would like to dedicate my thesis to my parents, Ronaldo Capaverde Silva and Rosane Andrade Batista, my siblings Mateus and Alice, and Elisabete Regina Silva da Costa.

# Chapter 1

## Introduction

The mixture of two or more liquids is something mundane in our daily activities, such as vinegar (mixture of water and acetic acid), the different components of some paints—the pigments and solvent [1]—or salad dressing. In the first application, the components are miscible, so the solution is stable. However, the latter two will eventually phase separate over time, causing the solution to lose its properties, including loss of color and taste, respectively. Therefore, the interaction between two liquids has been extensively studied in the scientific community, with the end goal to stabilize them temporarily for the forementioned applications.

## The Liquids' Polarity Origin

To understand why some liquid mix while others do not, it is important to know the concept of polarity and how it arises. For liquids, the main characteristic controlling the bond energy between liquids A and B is the polarity between them. This phenomenon arises from differences in electronegativities of the atoms in the bond [2]. The greater this difference, the more polar a liquid is. Water, for example, is a polar liquid because it is composed of one oxygen—whose electronegativity is 3.44— bonded to two hydrogens, whose electronegativity is 2.2. On the other hand, hydrocarbons are not polar because carbon's electronegativity is 2.55, making the difference between H-C negligible [3]. Therefore, we classify water as polar and hydrocarbons as non-polar, a crucial distinction for when mixing the two liquids.

## Miscibility between two liquids

According to the Gibbs free energy for mixing shown in the table 1 below, if we assume that there is no interaction between two liquids –in other words, the enthalpy of mixing between them is zero—the energy will always be lowered with a higher entropy, and therefore the natural tendency of the two liquids will be to mix to be at the lowest energy state possible [4]. However, most liquids exhibit some interaction in the molecular level between them, creating an extra energy in the equation: the bonding energy between the liquids.

**Table 1. Gibbs Free Energy Equation Possibilities**

| *Variables* | *Resulting Equation* | *Analysis* |
|---|---|---|
| $\Delta H_m > 0, \Delta S_m > 0$ | $\Delta G_m = \Delta H_m - T\lvert\Delta S_m\rvert$ | Mixing at high temperatures |
| $\Delta H_m < 0, \Delta S_m > 0$ | $\Delta G_m = -\Delta H_m - T\lvert\Delta S_m\rvert$ | Mixing at any temperature |
| $\Delta H_m > 0, \Delta S_m < 0$ | $\Delta G_m = \Delta H_m + T\lvert\Delta S_m\rvert$ | No mixing at any temperature |
| $\Delta H_m < 0, \Delta S_m < 0$ | $\Delta G_m = -\Delta H_m + T\lvert\Delta S_m\rvert$ | Mixing at low temperatures |

.

This extra bond energy is called enthalpy of mixing, and it can be positive or negative. If it is negative, it means that the bond energy between liquids A and B is lower than the average bond energy of the pure liquids. Therefore, the mixture will be homogeneous regardless of the temperature. However, if the reverse is true, the mixture may be heterogeneous depending on the temperature, with a higher temperature almost always tending for the mixture of the two liquids

being favorable [5]. As an example, since the type of bonding between hydrocarbons and water or other polar compounds are different, the mixture will be heterogeneous at lower temperatures, such as at room temperature for most of the oil-water systems[5].

## Difference in polarity leads to interfacial energy

In the case of a positive enthalpy of mixing, the difference in the type of bonding between the two liquids leads to a natural separation between the two surfaces, which is called interfacial force. This force acts in the interfacial area between the two liquids, creating an interfacial energy [6]. A higher polarity difference between the molecules will make the interfacial tension between them increase, leading to a more unstable system. Therefore, the system will always tend to decrease its total energy by minimizing the surface tension.

## Stabilizing the two liquids

To stabilize the different components in the solution by reducing the total energy of the system, one common approach is the use of surfactants, which are molecules that have a hydrophilic (affinity with water) and hydrophobic (aversion with water) part [7]. It is important to note the term stabilize in this context refers to kinetic stabilization, as overall the thermodynamic energy of the system is still lower if the components fully separate. As seen in Table 2, surfactant addition can reduce the surface tension substantially, making the system more stable [8]. Although this method is widely spread, it is also restrictive to each specific liquid-liquid solution, rendering it less effective in more complex systems [9].

**Table 2. Surface Tension Reduction Effect of Different Surfactants on a Water-Lotus Leaf System [8]**

| *Surfactant* | *Surface tension reduction (%)* |
|---|---|
| **10 mM SDS** | 56.49 |
| **10 mM TritonX-100** | 56.28 |
| **10 mM CTAB** | 66.53 |

Another less studied approach is to stabilize the liquids using particles. Although the introduction of the particle in the interface between both liquids creates two additional terms in the total energy equation as depicted in figure 1, the overall energy can still be reduced due to the minimizing of contact area between two liquids [9]. As an example, figure 1 depicts a particle immersed in an oil-oil interface. If the interfacial energy of the particle across both interfaces is sufficiently small so that the two additional terms can be considered insignificant, the total energy will be reduced by the physical area blocking of the particle in the interface.

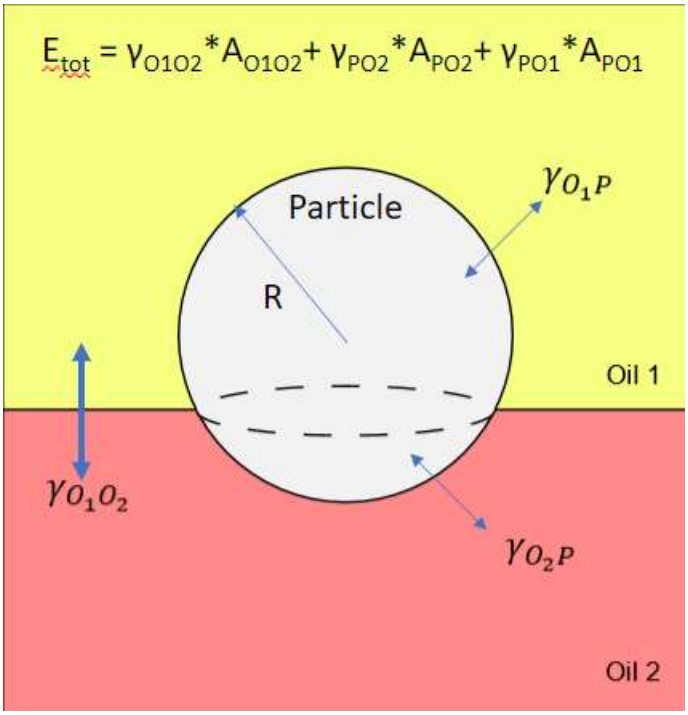


**Figure 1. Illustration of a Particle in an Oil-Oil Interface**

**The total interfaced energy for a perfectly spherical particle is displayed on the top of the figure, where $\gamma_{O1O2}$ , $\gamma_{PO2}$, and $\gamma_{PO1}$ represent the surface tension between oil 1 and oil 2, particle and oil 2, and particle and oil 1 , respectively and $A_{O1O2}$ , $A_{PO2}$ and $A_{PO1}$ represent the contact area between oil 1 and oil 2, particle and oil 2, and particle and oil 1, respectively.**

The effectiveness of the energy reduction depends on the total surface area that the particle can cover, which in term depends on the contact angle between the particle and the liquids. Using Young's equation, the angle formed by the particle in the interface is related to the difference in the interfacial tension of the particle with each interface divided by the interfacial tension across both liquids [10]. In other words, to maximize the particle coverage in the interface, the particle needs to be equally wetted in both liquids, as illustrated in the table 3 and figure 2, following the example from above.

**Table 3. Young's Equation for Balancing Surface Energies in the Particle-Liquid-Liquid Interface**

| *Young's Equation* | $\cos\theta = (\gamma_{PO1} - \gamma_{PO2})/\gamma_{O1O2}$ |
|---|---|
| If $\gamma_{PO1} < \gamma_{PO2}$ | $\theta < 90°$ |
| If $\gamma_{PO1} = \gamma_{PO2}$ | $\theta = 90°$ |
| If $\gamma_{PO1} > \gamma_{PO2}$ | $\theta > 90°$ |

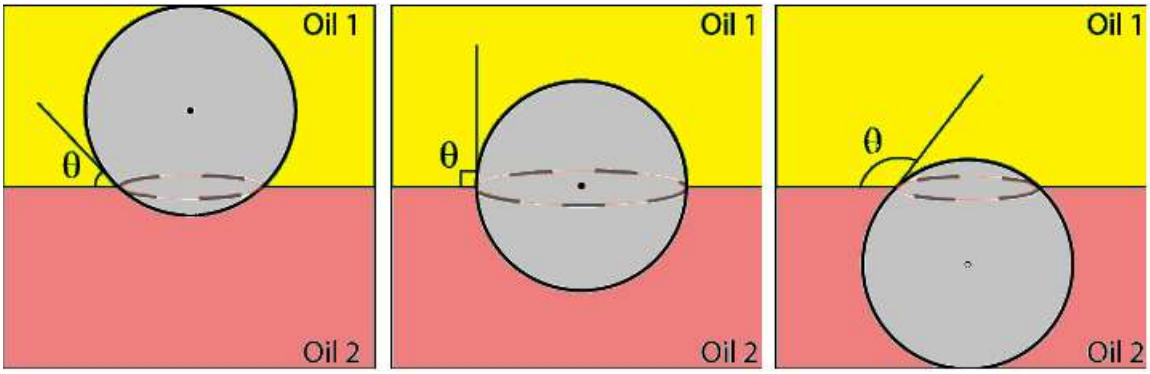


**Figure 2. Three Possible Particle Scenarios Arising from Table 3**

**From left to right: particle scenario where the θ angle is less than, equal, and greater than 90°.**

As seen before, it is possible to change the interfacial energy between the particle and the liquid –and therefore, the particle's coverage area—by modifying its end groups. A more hydrophobic end group –such as attaching hydrocarbons in the particle surface—will make the surface interaction between the particle with water and oil increase and decrease, respectively, making the particle more hydrophobic as well [11].

# Chapter 2

# Double Oil Reconfigurable Pickering Emulsion in Water

## Background Information

The system being studied comprises of three different liquids with the particle stabilizing the oil-oil interface. Therefore, it is important to understand the system's behavior without the influence of the particle. As seen in figure 3, the morphology of a hydrocarbon-fluorocarbon droplet on water depends on the interfacial tension interactions between the three liquids, best pictured by Neumann's triangle. When the interfacial tension between the two oils is low—such as in hexane-perfluorooctane (PFO)— one fully encapsulates the other depending on its interfacial tension with water: when using a surfactant that stabilizes fluorocarbons in water such as Capstone FS-30, that oil will be the one encapsulating the hydrocarbon, and vice-versa when using a hydrocarbon surfactant, such as sodium dodecyl sulfate (SDS). Upon increasing the interfacial tension between these two oils (such as increasing the hydrocarbon length), the morphology changes to a Janus droplet, as the overall interfacial energy is lowered when the oil partially contacts the water instead of being fully immersed in the other oil [12]. Therefore, it is possible to modify the morphology of the droplet by either changing the surfactant stabilizer between the water and the two oils or changing the oil compositions.

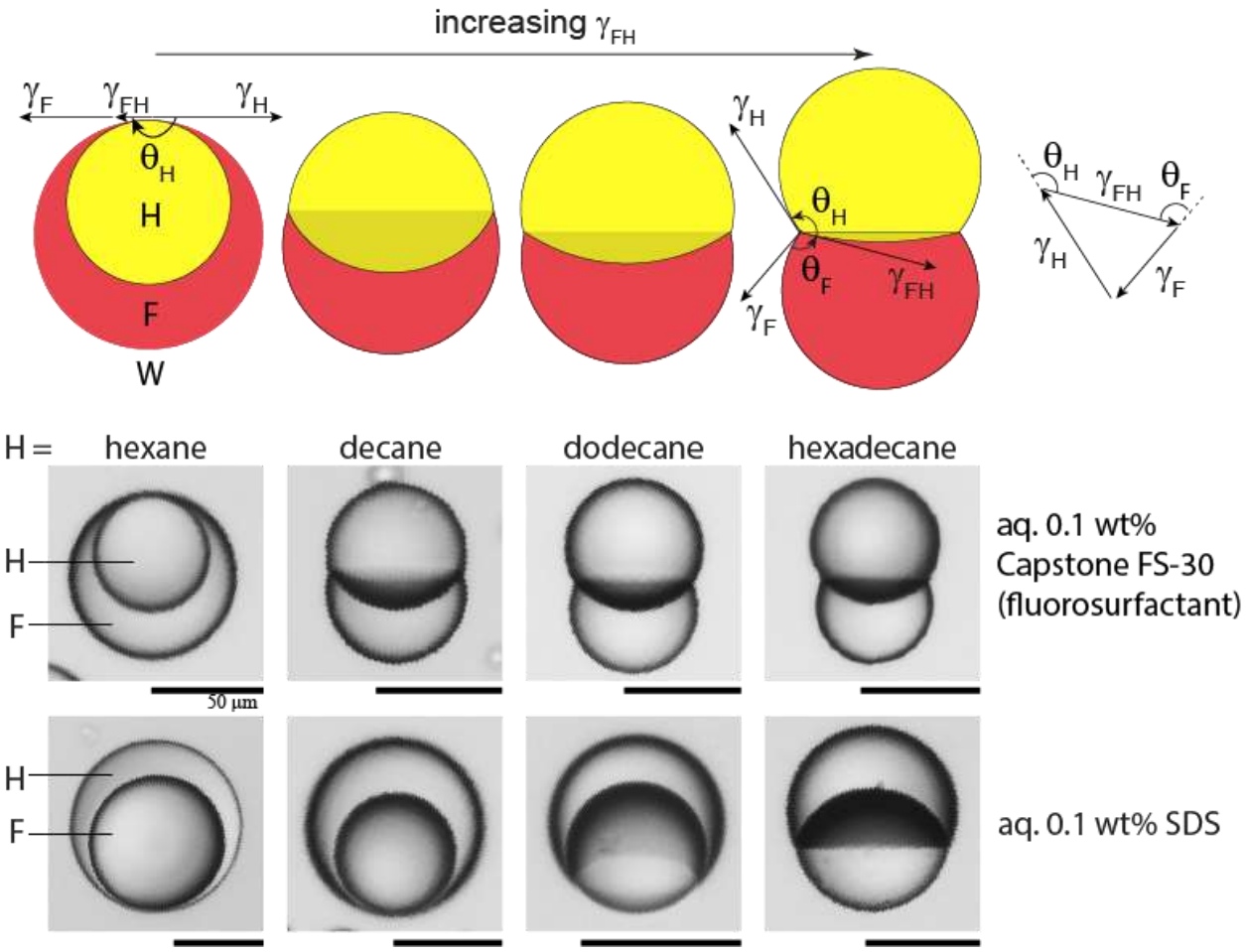


**Figure 3. Interfacial Increase Effect in Droplet Morphology**

**On the top of the figure, an illustration of the phenomena being observed experimentally. A balance in the interfacial tensions between the hydrocarbon oil (H), PFO (F) and water (W) is shown by the Neumann's triangle on the right. The experimental pictures depict the increase between the interfacial tensions between the two oils going from lowest (left) to highest (right) in two different surfactants with 0.1 wt% concentration in water: Capstone and SDS. All scale bars denote 50 µm. Partially reproduced from [12].**

Surfactants can be used to stabilize the water-oil interface and create several different morphologies; however, they cannot independently change the oil-oil interfacial tension, and therefore the morphology control is more limited [13]. If the interfacial tension between the oils

can be changed with the introduction of particles, there can be several new double oil configuration possibilities.

## Experimental Procedure

Materials: The fumed silica particles were provided by Wacker Chemie, with the S13 silica having no surface modification, and H20RH with a 75% surface coverage of long hydrocarbon chains. The chemicals used include hexadecyltrimethoxysilane (Aldrich, ≥85%), perfluorohexane (Synquest Laboratories, 98%), acetone (Fisher Scientific, 99.5%), hexane (Fisher Chemicals, 99%), toluene (VWR Chemicals, 99.5%), decane (TCI America, 99.0%), dodecane (Alfa Aesar, 99%), amongst others, with no further purification step.

Particle surface functionalization: The volume of each reagent is presented in the table 4 below. The general procedure involves mixing 250 mg of the particle in the solvent and making it well dispersed. After addition of the base and the silane, the mixture is sealed and put in a bath sonicator for 1h. The solution is diluted with acetone and centrifuged to remove impurities 3-4 times and then the particles were allowed to dry.

Emulsion preparation: The silica particles were well dispersed in one oil using a probe (QSonica Q700) sonicator, with a concentration of 1 wt/vol%. Oil-oil emulsions were created with equal volumes and emulsified using Vortex Genie 2 at 3200 rpm for 10 s in a dram glass vial. The emulsions were then added to an aqueous surfactant solution using a 1:2 volume ratio and emulsified using Vortex Genie 2.

**Table 4. Chemicals Used for Particle Synthesis**

| *Particle #* | *Particle type* | *Solvent (mL)* | *Silane (µL)* | *Base (µL)* |
|---|---|---|---|---|
| **1** | **S13** | **Acetone (10)** | **H-Silane (200)** | **$NH_4OH$ (100)** |
| **2** | **S13** | **Acetone (10)** | **H-Silane (600)** | **$NH_4OH$ (100)** |
| **3** | **S13** | **Acetone (10)** | **H-Silane (1000)** | **$NH_4OH$ (100)** |
| **4** | **S13** | **Acetone (10)** | **F-Silane (25)** | **$NH_4OH$ (100)** |
| **5** | **S13** | **Acetone (10)** | **F-Silane (75)** | **$NH_4OH$ (100)** |
| **6** | **S13** | **Acetone (10)** | **F-Silane (100)** | **$NH_4OH$ (100)** |
| **7** | **S13** | **Acetone (10)** | **F-Silane (150)** | **$NH_4OH$ (100)** |
| **8** | **H20RH** | **Perfluorohexane (6), Hexane (4)** | **F-Silane (400)** | **$C_4H_{11}N$ (200)** |
| **9** | **H20RH** | **Perfluorohexane (6), Hexane (4)** | **F-Silane (1000)** | **$C_4H_{11}N$ (200)** |
| **10** | **H20RH** | **Perfluorohexane (6), Hexane (4)** | **F-Silane (1200)** | **$C_4H_{11}N$ (200)** |
| **11** | **H20RH** | **Perfluorohexane (6), Hexane (4)** | **F-Silane (3000)** | **$C_4H_{11}N$ (200)** |
| **12** | **H20RH** | **N/A** | **N/A** | **N/A** |

## Results and Discussion

The first step is modifying the silica particle end groups to observe the effect in the oil-oil stabilization, which can be done by following the experimental procedure explained in the

previous section. As seen in figure 4, an increase in the hydrocarbon coverage (samples #1-3 and H20RH) have no effect in the oil-oil stabilization, as the two oils were completely separated in less than 15 min, with no stable emulsions. All the particles remained in the hexadecane phase, as their end groups are more attracted to it.

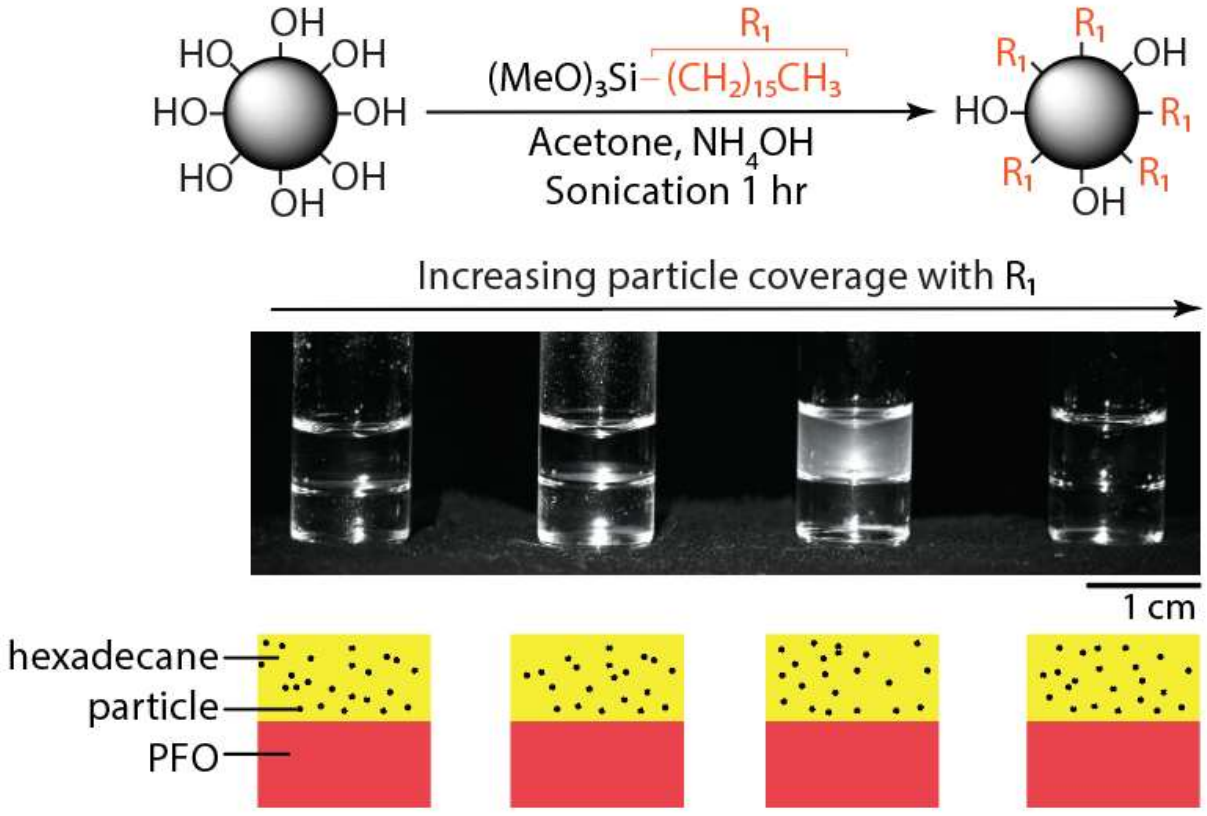


**Figure 4. Silica Functionalization with Hydrocarbon End Groups**

**On the top of the figure, an illustration of the particle functionalization step using the hexadecyl end group. On the middle, a picture of the solution between hexadecane and PFO after 15 min sitting still at the table. Particle end group coverage increases going from left to the right (particles #1-#3 from table 4 and H20RH). On the bottom, an illustration of the distribution of the particle in each oil phase. Partially reproduced from [12].**

Upon particle functionalization using a fluorinated end group shown in figure 5, two-oil stabilization is achieved, although there was a significant droplet coalescence into large and

irregular shapes due to particle jamming in the interface [14]. From the results in figures 4 and 5, surface functionalization using only one type of end group is not effective in stabilizing the oil-oil interface.

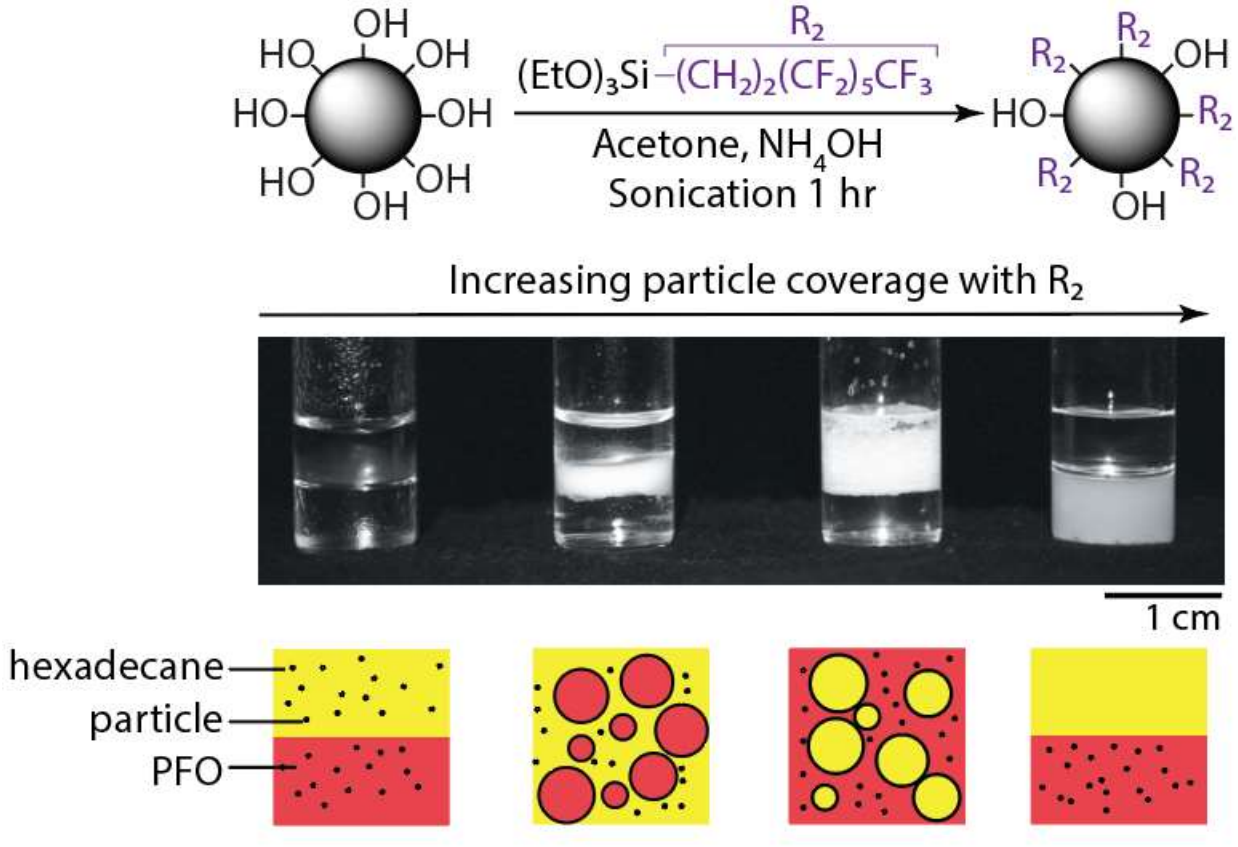


**Figure 5. Silica Functionalization with Fluorocarbon End Groups**

**On the top of the figure, an illustration of the particle functionalization step using the 1H,1H,2H,2H-perfluoroocty end group. On the middle, a picture of the solution between hexadecane and PFO after 15 min sitting still at the table. Particle end group coverage increases going from left to the right (particles #4-#7 from table 4). On the bottom, an illustration of the distribution of the particle in each oil phase. Partially reproduced from [12].**

Since one type of functionalization did not stabilize the oil-oil interface, the particles were functionalized with both end groups. Starting with the H20RH particle that already possess 75% of its surface with hydrocarbon end groups, further functionalization in the remaining

hydroxyl ends with fluorocarbons yielded the result seen in figure 6. The droplets remained stable for a period of more than two months, in which the photo was taken. The specific morphology of the droplet depended on where the particle dispersion was prior to the mixture of the two oils: the encapsulating oil would be the one where the droplets where first dispersed. That may be because of the particle pinning at the interface, trapping the particles in a meta-stable region [15].

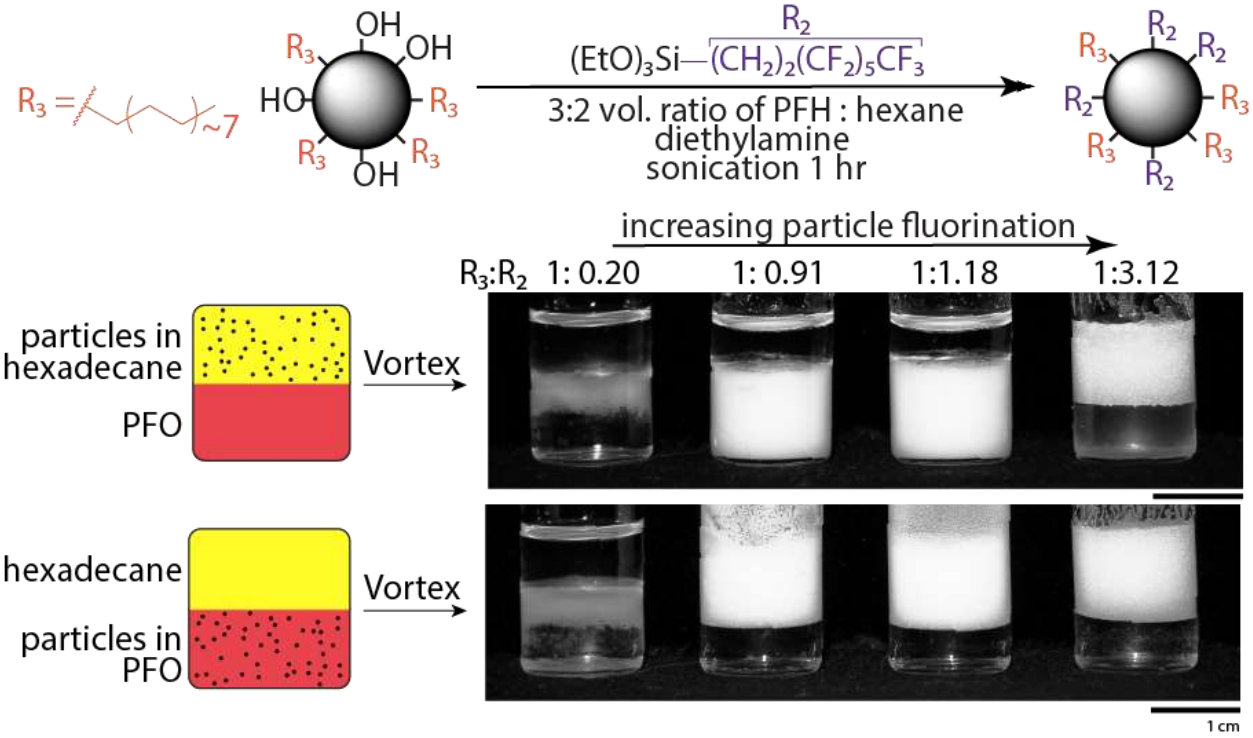


**Figure 6. Silica Particle with Hydrocarbon and Fluorocarbon End Groups Stabilization.**

**On the top row of the figure, an illustration of the particle functionalization step that already possesses hexadecyl end groups with the 1H,1H,2H,2H-perfluoroocty end group. On the other two rows, a picture of the solution after 2 months sitting still at the table, with the particles initially dispersed in either hexadecane or PFO. Particle end group coverage increases going from left to the right (particles #8-#11 on table 4). Partially reproduced from [12].**

Another important parameter to be considered is the particle concentration. As seen in figure 7, if the concentration is less than 0.5 wt% of the oil, there will be no droplet stabilization, as there are not enough particles in the interface to block the area between the two oils required for stabilization. Increasing the particle concentration diminished the droplet size while maintaining them spherical. These particles also worked in stabilizing PFO with a diverse range of oils (hexane, dodecane, isopropyl alcohol, amongst others), but were unable to stabilize the oil-water interface.

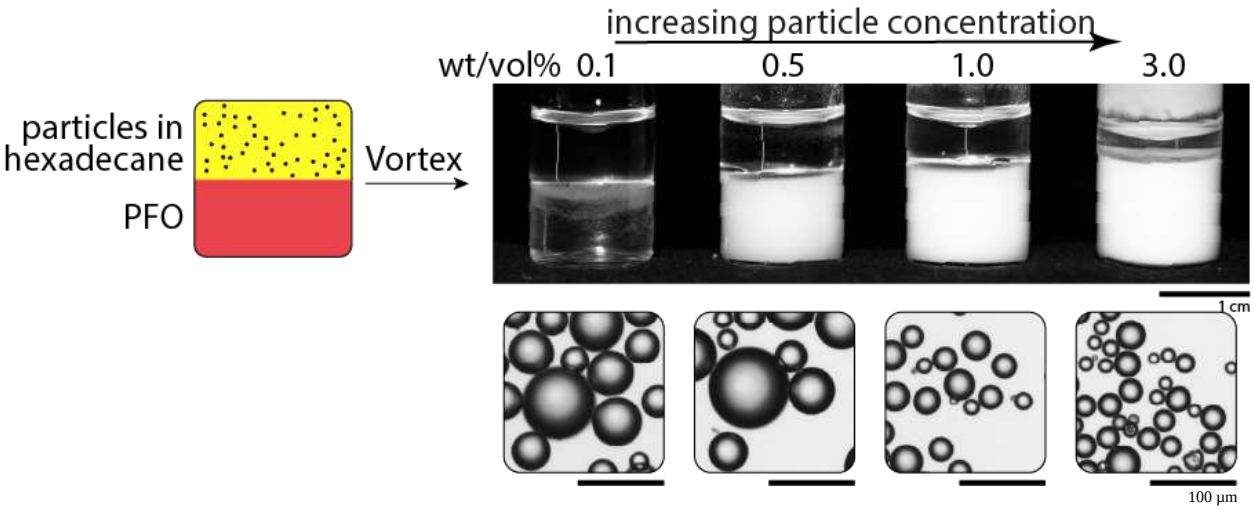


**Figure 7. Particle Concentration Effect on Droplet Formation**

**The effect of particle concentration is shown by increasing from left to right the wt/vol% of the particles (#9 on table 4) in hexadecane prior to bulk emulsification between hexadecane and PFO. The bottom row shows the respective optical micrographs of representative droplets from each vial, with all the scale bars at 100 µm. The photo was taken after 2 months of the vials sitting still at the table. Partially reproduced from [12].**

Since the particle was not able to stabilize the water-oil interface but was successful in oil-oil interface stabilization, the two methods were combined to produce stable double emulsions in water. To do that, the droplet solution obtained from the emulsification of the two

oils in figure 7 was added in the aqueous surfactant media, emulsifying it again to produce the oil-oil-water complex emulsions shown in figure 8. Most of the droplets were double emulsions (where one oil is completely encapsulated in another), although there were also higher order complex emulsions, single emulsions, and some Janus droplets, arising from the randomness of droplet creation from the bulk emulsification process [12]. As the droplets without particles shown in figure 3 were mostly Janus, there is compelling evidence that particles reduce the interfacial energy between the oils to create the double emulsion configuration.

In an attempt to mimic the switching between inner and outer encapsulating oil behavior when increasing the surfactant concentration that stabilizes the inner oil in a surfactant-only solution [15], each sample had the surfactant concentration flipped from SDS to Capstone and vice-versa. As seen in figure 8, the starting double emulsions did not change their configuration at all, while the Janus droplets changed shape but never got fully encapsulated, which is another supporting evidence for particles being stuck in the interface between oil-oil in case of the double emulsion and oil-oil-water in case of the Janus ones.

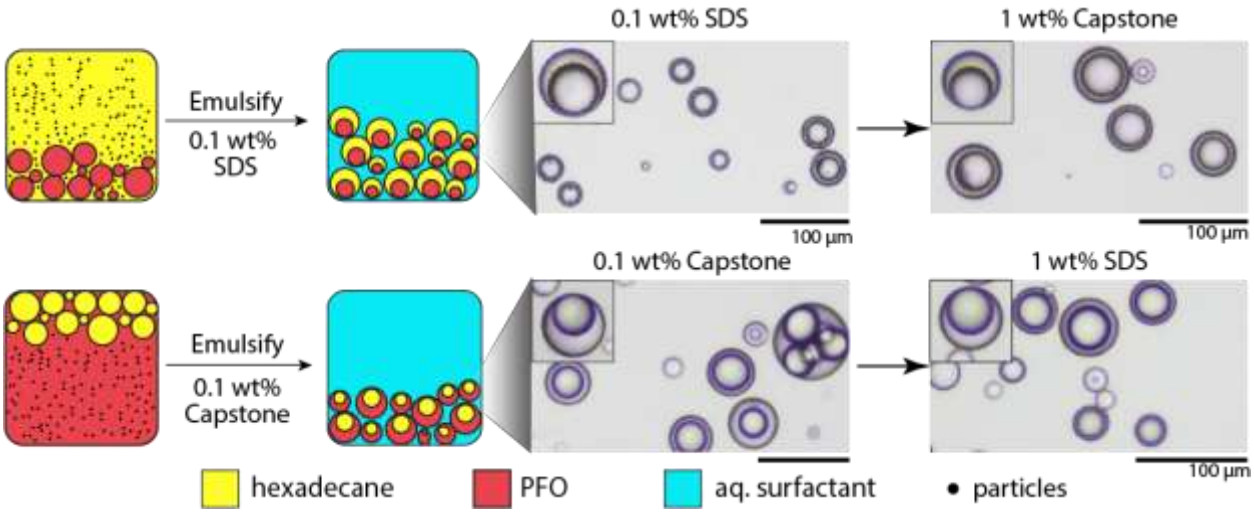


**Figure 8. Water-Oil-Oil Complex Emulsions**

**Water-oil-oil complex emulsion formation by taking the mixtures obtained from figure 6, adding aqueous surfactant, and bulk emulsifying the resulting solution. On the top row, 0.1 wt% SDS in water is used to stabilize hexadecane, while 0.1 wt% Capstone in water is used to stabilize PFO on the bottom row. After the emulsions were formed, the complimentary surfactant was added in the solution to try flipping the outer oil phase (i.e., 1 wt% Capstone was added to the 0.1 wt% SDS solution, and vice-versa). No outer-phase switch was observed. All the scale bars at 100 µm. Partially reproduced from [12].**

# Chapter 3

# Self-Propulsion Enhancement of Oil Droplets in Aqueous Surfactant Using Particles

## Background Information

Often in nature there is occurrence of a chemotaxis phenomenon, where for example a white cell chases down the unwanted organism by their chemical trace [16]. It is possible to model that using symmetrical droplets in an aqueous surfactant media, although the specific mechanism for droplet movement is yet unknown in the literature. Current research points to the motion being driven by solubilization through micelles[17] or Marangoni flow from the interfacial reactions in the droplet[18], and some systems might have a combination of both[19]. A brief description of these phenomena is depicted below.

Micelle formation occurs when the surfactant concentration is above the critical micelle concentration [20]. Past that point, the surfactant molecules in water forms clumps with the hydrophobic tail towards inside of the clump and the hydrophilic head in the to reduce the interfacial energy between the hydrophobic part of the surfactant and water. The precise mechanism to oil solubilization into these micelles is poorly understood [21], although there are three main mechanisms discussed in the literature: direct deposition of oil into the aqueous media and then to micelles, micelle formation straight from the interface of the oil with water, and collision of micelle with the oil [22,23]. Nevertheless, micelles contribute to an increase in solubilization of the droplet, which may affect its speed.

Marangoni flow can be described as the fluid flow induced by a gradient in surface tension at a fluid-fluid interface [24]. This gradient could arise from the solubilization from the

oil into the surfactant, creating a weaker (less oil-water stabilizing) surfactant, as the micelle is partially filled up with the oil. With a reduced stabilization power, there will be temporarily a region with a higher surface tension, which creates a gradient, as in the other side of the droplet will remain with the original surface tension [25]. Upon this creation of an interfacial tension gradient, figure 9 shows the mechanism for droplet movement. The water will move from the region of lower interfacial tension to stabilize the higher interfacial tension region, which will induce the droplet to move forward. Furthermore, the surfactants in the front of the droplet will be fresh, while the back of the droplet will likely have exhausted surfactants due to the water movement carrying these surfactants that have had time to interact with the oil, making the droplet's movement continuous as long as this surface tension maintains asymmetry.

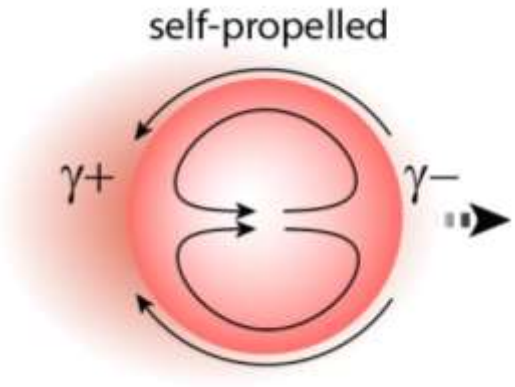


**Figure 9. Marangoni Flow Illustration**

**Illustration of an oil droplet in an aqueous surfactant media. The γ+ and γ- represent a greater and lower interfacial tension, respectively. The red trail also represents this difference in interfacial tensions, creating a gradient between the front and the back of the droplet, and making it move towards the direction of the arrow due to Marangoni flow effects.**

If the particles stay at the oil-water interface, there can be a permanent asymmetry introduced in the droplet depending on the particle motion inside the droplet and its interaction

with the aqueous media. With that hypothesis in mind, particles were introduced into the droplets to create this permanent asymmetry. Results point to a droplet speed increase across several oils, including self-propulsion movement in droplet systems that were not originally mobile. With that in mind, there is a broadening of possible applications of active droplets and active droplet research by allowing more mobile oil droplets in aqueous surfactant systems.

## Experimental Procedure

Materials: The fumed silica particles were provided by Wacker Chemie, with the S13 silica having no surface modification, and H20RH with a 75% surface coverage of long hydrocarbon chains. The chemicals used include sodium dodecyl sulfate (SDS) (Sigma Aldrich, 99%), cetyltrimethylammonium bromide (CTAB) (Sigma Aldrich)acetone (Fisher Scientific, 99.5%), Fluorescein sodium salt (Fluka), bromohexadecane (TCI, 96%), N-hydroxysuccinimide (NHS) (Chem Impex Int'l, 99.5%), amongst others, with no further purification step.

Fluorescent particle surface functionalization: The complete process is illustrated in figure 10 below. Approximately 250 mg of silica particle were well dispersed in 10 mL of acetone in a 25 mL flask. Upon the addition of 100 µL of 30 wt% ammonium hydroxide and 300 µL of APTES, the flask was closed, and bath sonicated for 1 h. The resulting solution was diluted in 30 mL of acetone and centrifugated at 7100 RPM for 10 min. This last step was repeated 2 more times, and the particles were dried overnight and put in a 25 mL of 2-(N-morpholino)ethanesulfonic acid (MES) buffer (with the pH of 5 and molarity of 0.5). In a 250 mL flask, 125 mL of MES buffer was added along with 165.9 mg of Ethylene dichloride (EDC), 342.1 mg of fluorescein sodium salt, and 246 mg of NHS. After complete dissolution, the

particles were added into the 125 mL flask, which was then sealed, covered in aluminum foil, and left to react for 24 h while stirring. The solution was then cleansed by diluting in 30 mL of acetone and centrifugating at 7100 RPM for 10 min. This cleaning step was repeated 4 more times, and the particles were dried overnight. To make the particles hydrophobic, they were well dispersed in 10 mL hexane and added to a 25 mL flask. Upon the addition of 200 mL of diethylamine and 1.5 mL of hexadecyltriethoxysilane, the flask was sealed, foiled, and stirred for 24 h. The same cleansing process was repeated to achieve the final fluorescent hydrophobic fumed silica particles.

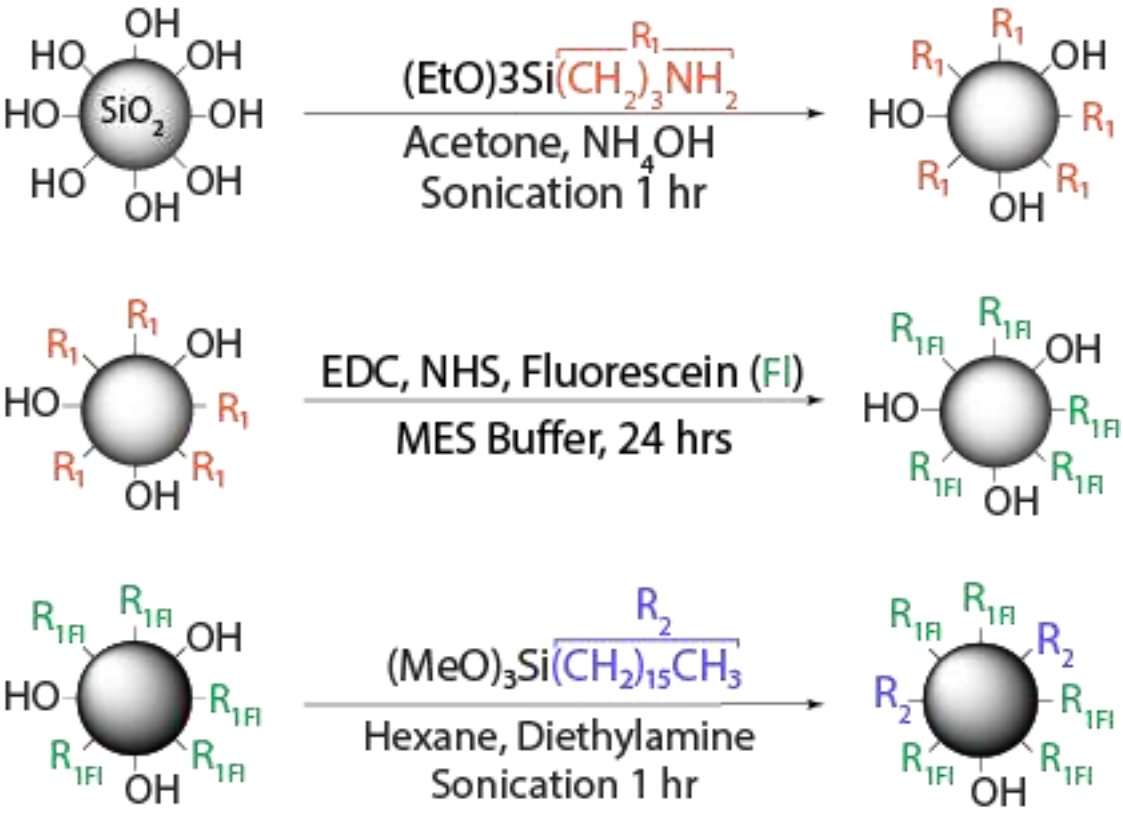


**Figure 10. Fluorescent Hydrophobic Particle Transformation**

**Process depicting the silica S13 particle fluorescence and subsequent functionalization. Each row represents a step in the particle modification, starting with the amine end group introduction, that is substituted with fluorescein end groups, and the remaining unfunctionalized groups are substituted by a hydrocarbon end group. Partially reproduced from [26].**

Emulsion preparation: Silica particles were well dispersed in the oil using a probe sonicator and immediately mixed with the aqueous surfactant using a Vortex Genie 2 at 3200 rpm for 4 s.

Surface particle coverage analysis: The surface coverage was determined using fluorescent images of the particles, such as in figure 11. The surface coverage was approximated to be a symmetric cap of particles. There is an inherent error in the estimation, as the particle does not necessarily need to be at the surface and the coverage does not match the entire span of

the designated height, but nonetheless this provides a good ballpark range for qualitative interpretation.

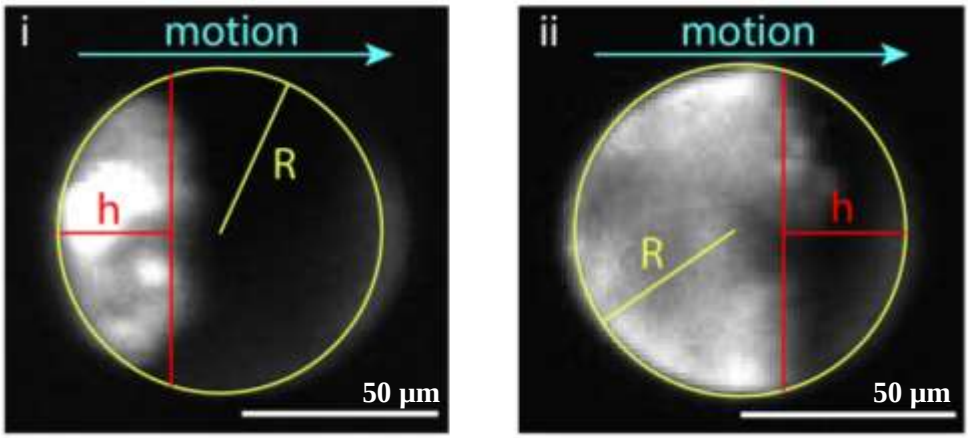


**Figure 11. Particle Coverage Example**

**Pictures obtained from the fluorescent particles in the droplets. From the image, it is possible to acquire the radius of the particle and the height of the particle coverage, as depicted in figure 11. From that, it is possible to estimate the particle coverage by dividing the height by the droplet's diameter. For i, the coverage is 29 µm/90 µm = 32%, and for ii the coverage is 1-42 µm/60 µm = 70%. Some key assumptions in making this calculation are the particles cover all area before h (including the z axis, which we cannot obtain from the 2d image) and the droplet has a perfectly spherical shape. Partially reproduced from [26].**

Analysis of droplet speed: The droplets were put in the dish containing the surfactant solution. After gently agitation to disperse the droplets, the videos were taken using a 6x magnification, 1024x1024 resolution, and 30 fps with the Andor Zyla 4.2P camera. Droplet speed was analyzing using a MATLAB code program [19,27] that tracked the droplet positions at each frame at the video, with an example shown in figure 12. The average speed was obtained by averaging all droplet maximum speeds captured in each video, with the data values being the average maximum speed and the standard deviation of the maximum speed. The drift velocity from convection was not considered, as the value is insignificant compared to the droplet speeds.

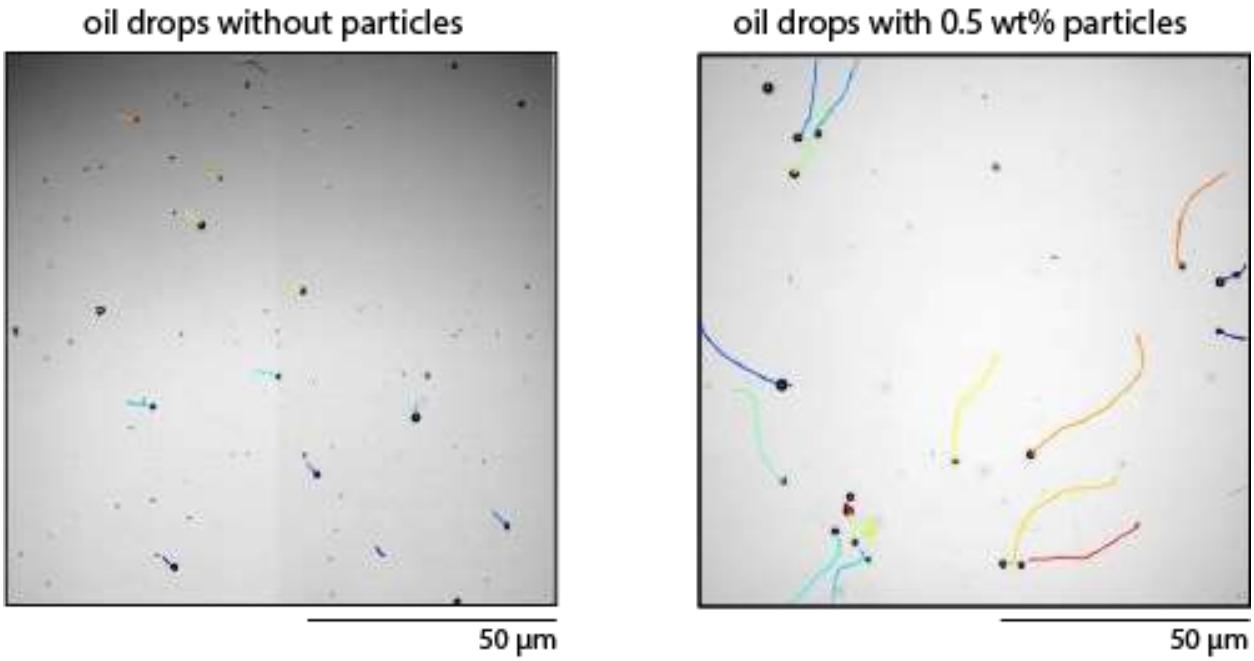


**Figure 12. Droplet Position Tracking Example**

**A droplet dislocation picture created by the MATLAB code after video analysis of bromodecane oil droplets in water containing 0.1 wt% Triton-X—with no particles in the left image and 0.5 wt% H13L silica in the right image—in a period of 1 min. There is no noticeable movement from the droplets without particles, while the displacement of the droplets with particles is noticeable. From the displacement and time, it is possible to obtain the droplet speeds across the time span. Partially reproduced from [26].**

## Results and Discussion

The initially studied system was composed of bromodecane in Triton-X with water, as the droplets were already self-propelled before the introduction of the particle and bromodecane sinks in water, which removes the height translation for the speed calculations which cannot be captured by a video in two dimensions. The H13L particles wet both oil in water, so they have a preference to staying in the liquid interface. As can be seen from figure 12, the droplet trajectories were mostly curved, so the speed values acquired for the speed analysis were the

individual top speed of each droplet, as that is the more likely value to represent the true speed (without deceleration effects caused by the curve trajectories).

In figure 13 it is possible to observe the influence of the particle in the droplet speed over three different surfactant concentrations. As expected from results in literature, an increase in surfactant increases the droplet speeds due to the micelle-mediated propulsion mechanism [19]. The most interesting phenomena is the increase of droplet speeds upon particle addition regardless of the surfactant concentration, with an impressive order of magnitude difference in the case of 0.1 wt% Triton-X 100. The speed enhancement peaks around 0.4 wt% H13L in bromodecane, although the error bars are large. As the particle wt% further increases, there is a decrease in the droplet speed, at which point visual particle aggregation in the droplet's interface with water is observed.

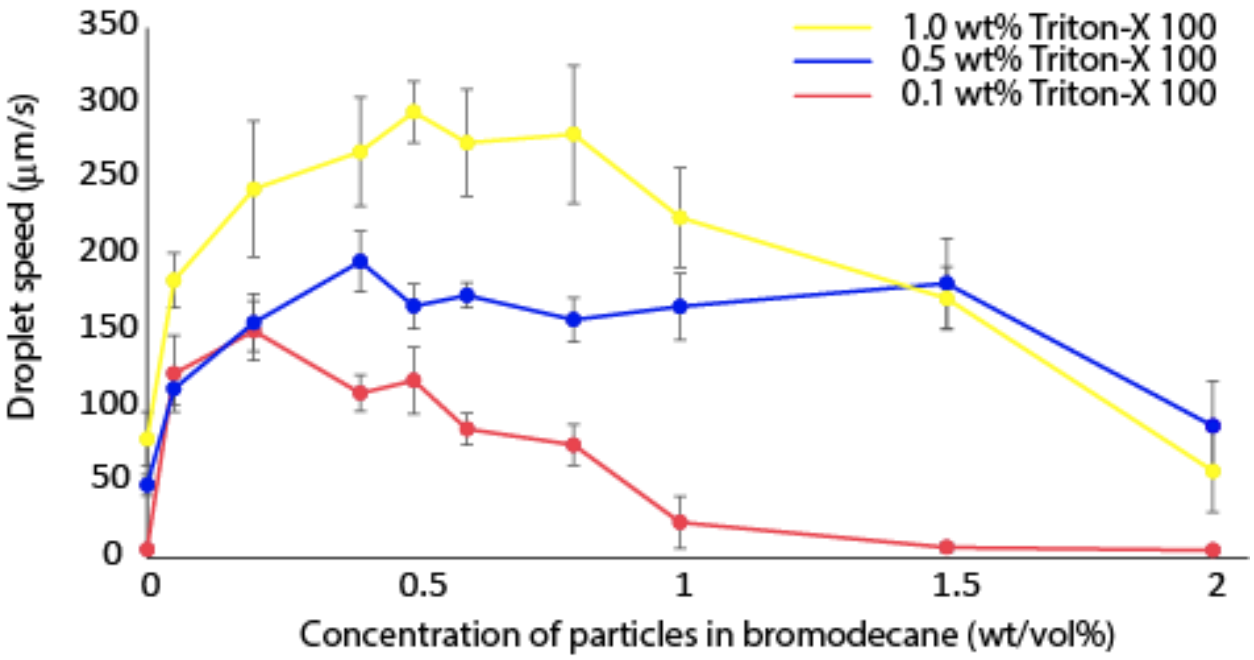


**Figure 13. Droplet Speed Across Different Particle Concentrations in Different Surfactant Concentrations**

**Bromodecane droplet maximum speed average and standard deviation gathered from the videos across different H13L particle concentrations in different aqueous Triton-X concentrations. At least 10 different droplet speeds are used per data point. Partially reproduced from [26].**

To better understand the source of such large standard deviations and why this speed trend is happening, H13L particles were substituted by S13 fluorescent ones to study the effect of surface coverage in the speed of the droplet. Although the method to calculate the particle coverage was not entirely accurate, figure 14 still gives qualitative insights into the phenomena happening. The first trend worth noticing is that the particle coverage distribution across a given initial particle concentration in oil is substantial. With lower particle concentrations, the mean particle coverage is also low, with an increase in the mean coverage as the particle concentration goes up. However, there is a spread in terms of how many particles are inside each droplet due to the bulk emulsification method, which gives rise to different particle coverages and,

consequently, a higher standard deviation of speeds. Nonetheless, there is a clear trend between particle coverage and speed: a lower particle coverage correlates with lowers droplet speeds, with a speed peak around when there is around 40% particle coverage, eventually dropping to zero with further particle coverage in the interface.

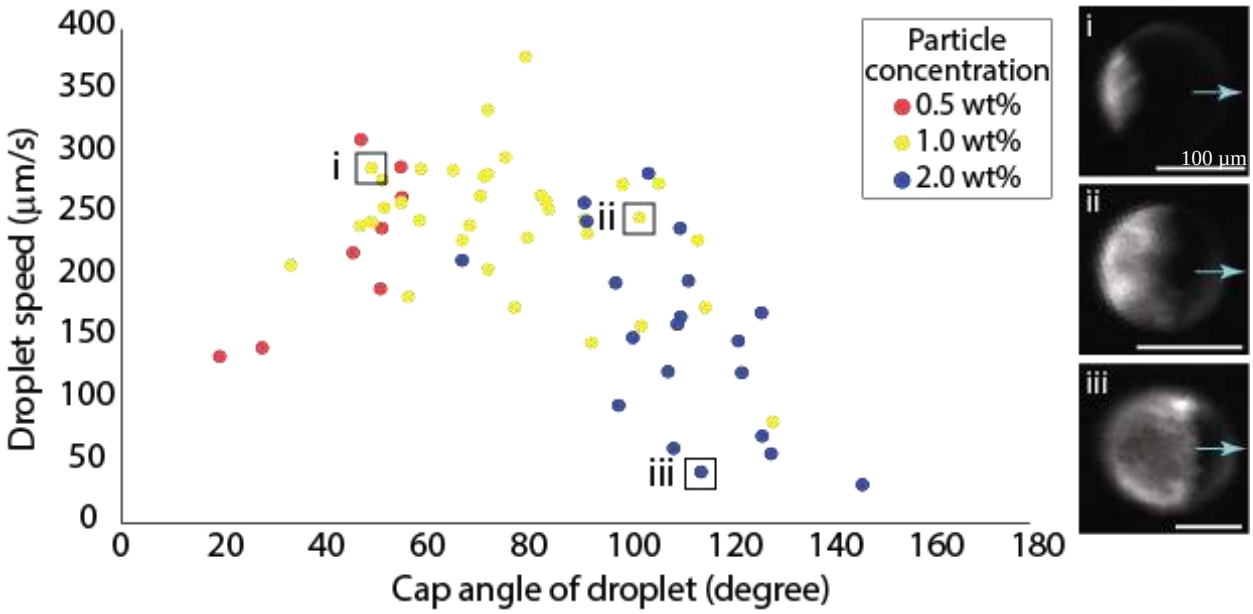


**Figure 14. Particle Coverage Vs Speed**

**Individual droplet speeds plotted against the angle of the particle cap coverage. This angle is obtained by comparing the horizontal axis of locomotion to the most advanced visible particle in the image, with 180 being when the droplet is fully covered by particles. Partially reproduced from [26].**

To further confirm the hypothesis that the particle coverage was the reason for the droplet speed enhancement, the speed of a single bromodecane droplet was tracked along its movement life span. As it can be seen in figure 15, the droplet started with low particle coverage and a speed around 250 µm/s. As time passed by and the droplet solubilized, its size decreased, and the particle coverage increased. The speed remained stable until around 37 min, at which point it decreased significantly due to the particle's interfacial coverage value increasing past the ideal

value for maximum speed, and at the end of the experiment there was no movement at all, with the surface almost completely covered by particles.

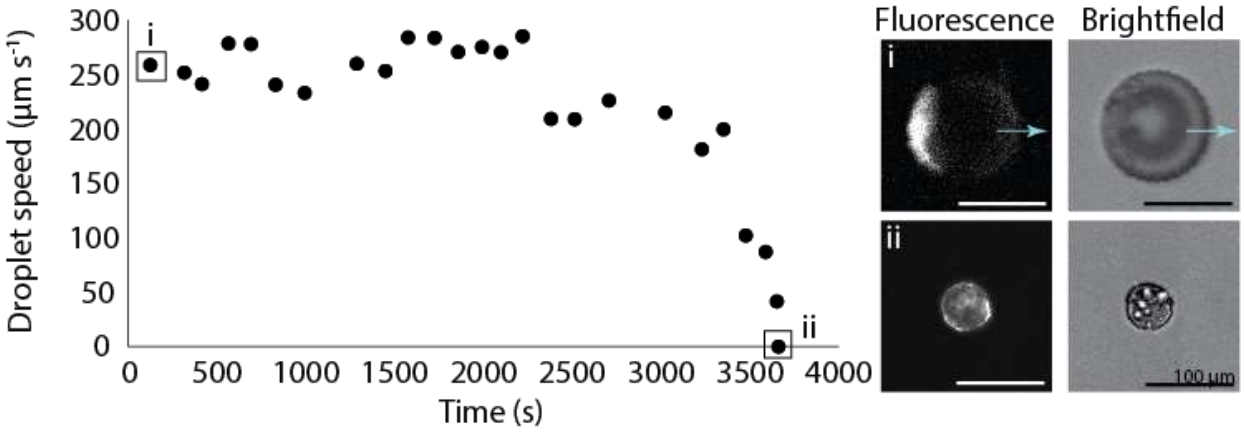


**Figure 15. Single Droplet Speed Tracking**

**Speed tracking of a 0.5 wt% H13L in bromodecane droplet in 0.5 wt% Triton X aqueous media across the lifespan of 1h. The particle started with a small concentration of particles in the back, but as time passed, it solubilized and decreased its oil volume, while maintaining the particle concentration, thereby increasing the particle's surface area in the droplet until it was fully covered. Partially reproduced from [26].**

All these results elucidate a possible mechanism for droplet speed enhancement due to the particles blocking the interface. Upon initial droplet perturbation enough to start the Marangoni flow process, the particle rearranges themselves in the back of the droplet as depicted in figure 16. With that new configuration, the surfactant is free to adsorb in the front of the droplet (in the direction of its movement), but the particles impede surfactant adsorption in the back of the droplet, raising the interfacial tension in that region even more than the scenario without particles. Therefore, the interfacial tension between the two sides of the droplet is greater if compared to the system without particles, making the Marangoni flow more substantial i.e., the droplet to move faster.

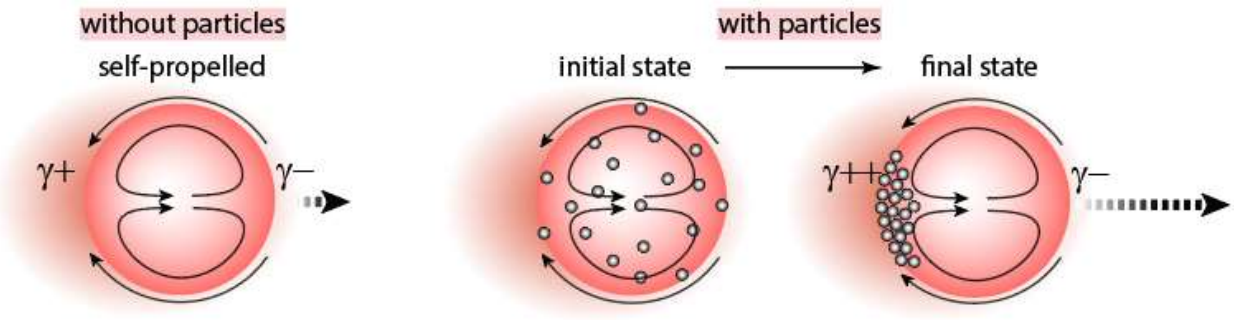


**Figure 16. Proposed Droplet Enhancement Illustration**

**Proposed mechanism for the particle speed enhancement. On the left, no particles on the system, so the normal Marangoni flow depicted in figure 9 happens. Upon addition of particles, the gradient of interfacial tension between the front and back becomes accentuated after rearrangement of particles to the back, enhancing the Marangoni flow effect.**

In order to assess the universality of the phenomena, figure 17 shows different surfactants being used in the bromodecane-water solution. There is an overall speed enhancement across all surfactants, with a noticeable increase for the SDS surfactant system.

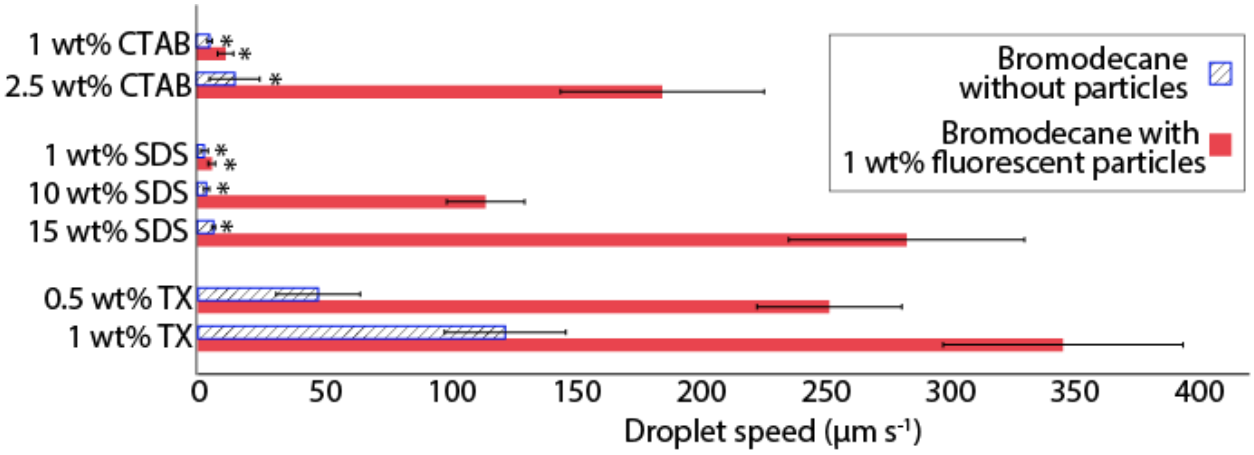


**Figure 17. Droplet Speed Enhancement Across Different Surfactants**

**Speed comparison between different aqueous surfactant systems using bromodecane with or without 1 wt% fluorescent particle. The blue and red bars represent the average highest speed of droplets without and with particles, respectively. The asterisk means the movement is likely from drifting instead of self-propulsion, as all droplets were moving to the same direction. The particles used are in the 30-50% particle coverage to account for possible differences in particle surface activity under the varying surfactant conditions[28]. Partially reproduced from [26].**

As Marangoni flow is a result of the interfacial gradient difference between water and the oil, different oil types with increasing hydrophobicity and different solubilization rates were assessed to compare the droplet speeds. As seen in figure 18, with the particle coverage between 30-50%, all oils except the vegetable oil showed a speed increase of the droplet. The slower speeds trends after bromodecane are likely from a slower dissolution rate of the oil in water [29], although there is still a big speed increase for bromohexadacane with particles.

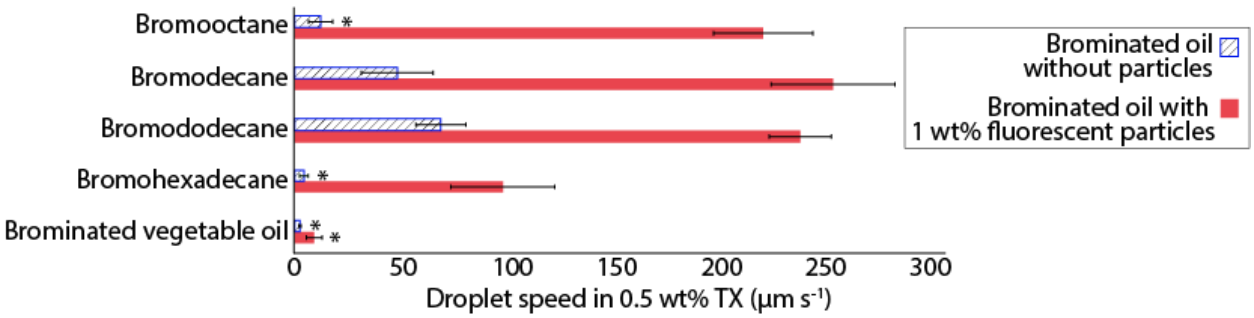


**Figure 18. Droplet Speed Enhancement Across Different Oils**

**Speed comparison between different oil droplets using 0.5 wt% Triton X as the aqueous media. The blue and red bars represent the average highest speed of droplets without and with particles, respectively. The asterisk means the movement is likely from drifting instead of self-propulsion, as all droplets were moving to the same direction. The particles used are in the 30-50% particle coverage to account for possible differences in particle surface activity under the varying surfactant conditions[28]. Partially reproduced from [26].**

# Chapter 4

# Conclusion and Future Work

In this work, the influence of a particle in the liquid-liquid interface was studied in two different scenarios: inner oil-oil stabilization creating complex and reconfiguring Pickering emulsions in water with surfactants and droplet speed enhancement upon addition of particle in the oil-aqueous surfactant media. A conclusion followed with some potential future research ventures for each study is detailed below.

## Double Oil Reconfigurable Pickering Emulsion in Water

In this study, there was successful fluorocarbon-hydrocarbon oil stabilization using particles due to its functionalization using both fluorophilic and lipophilic end groups. The Pickering emulsions were stable for extended periods of time, but the particles were unable to stabilize the water-oil interface as hypothesized. Therefore, by combining the methods of oil-oil particle stabilization and oil-water surfactant stabilization, double emulsions in water were achieved. This complex shape, amongst several different possible morphologies using the bulk emulsification method, arises from the combination of particles only stabilizing the oil-oil interface while surfactants reducing the energy between the outer oil and water. Future work may include a more thorough investigation on the particle jamming occurring in the oil-oil-water three-point contact line, trying to circumvent this high energy barrier required to remove the particle stuck in that three liquid interface and allowing a complete switch between the inner oil and outer oil. Furthermore, different end group functionalizing may expand the oil type double

emulsion creation, so different components can be mixed in the solution, allowing for more variety in the geometry configurations.

## Self-Propulsion Enhancement of Oil Droplets in Aqueous Surfactant Using Particles

In this study, a clear correlation between droplet speed increase and oil particle concentration was demonstrated. This speed enhancement is likely due to the surface coverage of the particles in the oil-water interface, which increases the interfacial tension disparity between the two liquids locally at that region and creates a greater surface tension gradient between the front and back of the droplet, enhancing Marangoni flow effects. This explanation is supported by the gradual increase in droplet speed up to around 40% particle coverage, at which point it starts to decrease because of a decrease in the surface tension gradient between the two sides. The generalization of this phenomena across different surfactants and oil. Future work may include the use of fluid mechanical models to explain this qualitative observation and calculate droplet theoretical speeds including factors such as particle roughness and mass.

## BIBLIOGRAPHY


1) Walter, P.; de Viguerie, L. Materials Science Challenges in Paintings. Nat. Mater. 2018, 17 (2), 106–109. https://doi.org/10.1038/nmat5070.
2) Raub, S.; Jansen, G. A Quantitative Measure of Bond Polarity from the Electron Localization Function and the Theory of Atoms in Molecules. Theoretical Chemistry Accounts: Theory, Computation, and Modeling (Theoretica Chimica Acta) 2001, 106 (3), 223–232. https://doi.org/10.1007/s002140100268.
3) Hendry, D. G.; Russell, G. A. Solvent Effects in the Reactions of Free Radicals and Atoms. IX. Effect of Solvent Polarity on the Reactions of Peroxy Radicals. J. Am. Chem. Soc. 1964, 86 (12), 2368–2371. https://doi.org/10.1021/ja01066a014.
4) Zhu, H.; Li, R.; Wang, F.; Chen, N.; Li, Z.; Wang, Z. Poly Tris (1-Imidazolyl) Benzene Ionic Liquids/Poly (2,6-Dimethyl Phenylene Oxide) Composite Membranes for Anion Exchange Membrane Fuel Cells. J Mater Sci 2017, 52 (18), 11109–11119. https://doi.org/10.1007/s10853-017-1270-8.
5) Silverstein, T. P. The Real Reason Why Oil and Water Don't Mix. J. Chem. Educ. 1998, 75 (1), 116. https://doi.org/10.1021/ed075p116
6) Hezave, A. Z.; Dorostkar, S.; Ayatollahi, S.; Nabipour, M.; Hemmateenejad, B. Investigating the Effect of Ionic Liquid (1-Dodecyl-3-Methylimidazolium Chloride ([C12mim] [Cl])) on the Water/Oil Interfacial Tension as a Novel Surfactant. Colloids and Surfaces A: Physicochemical and Engineering Aspects 2013, 421, 63–71. https://doi.org/10.1016/j.colsurfa.2012.12.008.

7) Tadros, T. Surfactants. In Encyclopedia of Colloid and Interface Science; Tadros, T., Ed.; Springer: Berlin, Heidelberg, 2013; pp 1242–1290. https://doi.org/10.1007/978-3-642-20665-8_40.

8) D. Y. Patil et al. Drop Collapse Assay on Lotus Leaf (Nelumbo Nucifera): A Simple and Cost-Effective Method for Rapid Detection of Biosurfactants. JEBAS 2016, 4 (5), 505–511. https://doi.org/10.18006/2016.4(5).505.511.

9) Chevalier, Y.; Bolzinger, M.-A. Emulsions Stabilized with Solid Nanoparticles: Pickering Emulsions. Colloids and Surfaces A: Physicochemical and Engineering Aspects 2013, 439, 23–34. https://doi.org/10.1016/j.colsurfa.2013.02.054.

10) Adam, N. K. Use of the Term 'Young's Equation' for Contact Angles. Nature 1957, 180 (4590), 809–810. https://doi.org/10.1038/180809a0

11) Xiao, M.; Xu, A.; Zhang, T.; Hong, L. Tailoring the Wettability of Colloidal Particles for Pickering Emulsions via Surface Modification and Roughness. Front. Chem. 2018, 6, 225. https://doi.org/10.3389/fchem.2018.00225.

12) Cheon, S. I.; Batista Capaverde Silva, L.; Ditzler, R.; Zarzar, L. D. Particle Stabilization of Oil–Fluorocarbon Interfaces and Effects on Multiphase Oil-in-Water Complex Emulsion Morphology and Reconfigurability. Langmuir 2020, 36 (25), 7083–7090. https://doi.org/10.1021/acs.langmuir.9b03830.

13) Huo, L.; Liu, G.; Yang, X.; Ahmad, Z.; Zhong, H. Surfactant-Enhanced Aquifer Remediation: Mechanisms, Influences, Limitations and the Countermeasures. Chemosphere 2020, 252, 126620. https://doi.org/10.1016/j.chemosphere.2020.126620.

14) Shi, S.; Russell, T. P. Nanoparticle Assembly at Liquid–Liquid Interfaces: From the Nanoscale to Mesoscale. Adv. Mater. 2018, 30 (44), 1800714. https://doi.org/10.1002/adma.201800714.

15) Zanini, M.; Marschelke, C.; Anachkov, S. E.; Marini, E.; Synytska, A.; Isa, L. Universal Emulsion Stabilization from the Arrested Adsorption of Rough Particles at Liquid-Liquid Interfaces. Nat Commun 2017, 8 (1), 15701. https://doi.org/10.1038/ncomms15701.

16) Lauga E. and Powers T. R. 2009 *Rep. Prog. Phys.* **72** 096601

17) Hanczyc, M. M.; Toyota, T.; Ikegami, T.; Packard, N.; Sugawara, T. Fatty Acid Chemistry at the Oil−Water Interface: Self-Propelled Oil Droplets. J. Am. Chem. Soc. 2007, 129 (30), 9386–9391. https://doi.org/10.1021/ja0706955.

18) Toyota, T.; Maru, N.; Hanczyc, M. M.; Ikegami, T.; Sugawara, T. Self-Propelled Oil Droplets Consuming "Fuel" Surfactant. J. Am. Chem. Soc. 2009, 131 (14), 5012–5013. https://doi.org/10.1021/ja806689p.

19) C. H. Meredith, P. G. Moerman, J. Groenewold, Y. J. Chiu, W. K. Kegel and A. van Blaaderen, et al., Predator–prey Interactions Between Droplets Driven by Non-reciprocal Oil Exchange, Nat. Chem., 2020, 12(12), 1136–1142, DOI: 10.1038/s41557-020-00575-0.

20) B. P. Binks, J. H. Clint, P. D. I. Fletcher, and, S. Rippon, , S. D. Lubetkin and, P. J. Mulqueen. Kinetics of Swelling of Oil-in-Water Emulsions Stabilized by Different Surfactants. *Langmuir* **1999,** *15* (13) , 4495-4501. https://doi.org/10.1021/la990054q

21) C. Kriegel, K. M. Kit, D. J. McClements and J. Weiss . Nanofibers as Carrier Systems for Antimicrobial Microemulsions. Part I: Fabrication and Characterization. *Langmuir* **2009,** *25* (2) , 1154-1161. https://doi.org/10.1021/la803058c

22) Long Xu, Zhe Qiu, Houjian Gong, Chenguang Liu, Yajun Li, Mingzhe Dong. Effect of diutan microbial polysaccharide on the stability and rheological properties of O/W nanoemulsions formed with a blend of Span20-Tween20. *Journal of Dispersion Science and Technology* **2018,** *39* (11) , 1644-1654. https://doi.org/10.1080/01932691.2018.1461636

23) Weiss, J.; Coupland, J. N.; McClements, D. J. Solubilization of Hydrocarbon Emulsion Droplets Suspended in Nonionic Surfactant Micelle Solutions. J. Phys. Chem. 1996, 100 (3), 1066–1071. https://doi.org/10.1021/jp9524892.

24) Schmitt, M.; Stark, H. Marangoni Flow at Droplet Interfaces: Three-Dimensional Solution and Applications. Physics of Fluids 2016, 28 (1), 012106. https://doi.org/10.1063/1.4939212.

25) Schmitt, M.; Stark, H. Swimming Active Droplet: A Theoretical Analysis. EPL 2013, 101 (4), 44008. https://doi.org/10.1209/0295-5075/101/44008.

26) Cheon, S. I.; Silva, L. B. C.; Khair, A. S.; Zarzar, L. D. Interfacially-Adsorbed Particles Enhance the Self-Propulsion of Oil Droplets in Aqueous Surfactant. Soft Matter 2021, 17 (28), 6742–6750. https://doi.org/10.1039/D0SM02234A.

27) Crocker, J. C.; Grier, D. G. Methods of Digital Video Microscopy for Colloidal Studies. Journal of Colloid and Interface Science 1996, 179 (1), 298–310. https://doi.org/10.1006/jcis.1996.0217.

28) Katepalli, H.; Bose, A. Response of Surfactant Stabilized Oil-in-Water Emulsions to the Addition of Particles in an Aqueous Suspension. Langmuir 2014, 30 (43), 12736–12742. https://doi.org/10.1021/la502291q.

29) Zhong, H.; Yang, L.; Zeng, G.; Brusseau, M. L.; Wang, Y.; Li, Y.; Liu, Z.; Yuan, X.; Tan, F. Aggregate-Based Sub-CMC Solubilization of Hexadecane by Surfactants. RSC Adv. 2015, 5 (95), 78142–78149. https://doi.org/10.1039/C5RA12388G.

**ACADEMIC VITA**

# Leonardo Batista Capaverde Silva

XXXXXXXXXXXXX | (XXX) XXX-XXXX | leocapaverde@gmail.com

## Objective

- To develop fundamental research towards solving humanity's environmental problems on energy, with a focus on both experimental and computational modeling.

## Education

**B.S IN MATERIAL SCIENCE AND ENGINEERING | 2018 - 2022 | THE PENNSYLVANIA STATE UNIVERSITY**

- GPA: X.XX
- Minor: Mathematics
- Related coursework: Computational materials science and engineering || Crystal Chemistry || Deep Learning Algorithms and Analysis

## Work Experience

**ATTENDANCE COORDINATOR | WORLD IN CONVERSATION | 01/2020 – PRESENT**

- Improved reliability and information gathering of filing system, from over 50 errors to 5 in each semester
- Developed a code that double checks the attendance records in three different documents
- Administered over 300 student records weekly

## Research Experience

**LAB ASSISTANT | DR. LAUREN ZARZAR GROUP ON EMULSIONS AND LASER PATTERNING | 08/2018 – PRESENT**

- Created over 200 soft matter experiments each semester
- Investigated the influences of particles at interfaces of the oil/oil system
- Developed a system to track droplets using MATLAB
- Second author in two published papers

**LAB ASSISTANT | DR. MOLINA HIGGINS GROUP | 08/2021 - PRESENT**

- Investigated the degradation of PET nanoparticles in water under the irradiation of X-rays
- Poster presentation in TMS 2022 conference in February 2022

## Honors/Awards

**SCHREYER'S HONORS || PHI KAPPA PHI HONORS || EMSAGE LAUREATE || ERICKSON DISCOVERY GRANT**

## Skills

**MATLAB, JAVASCRIPT, PYTHON || CONVERSATIONAL SPANISH || FLUENT PORTUGUESE AND ENGLISH**